Inorganic Chemistry

Article

pubs.acs.org/IC

On the Structure of β-Molybdenum Dichloride

Frederic Poineau,*[,†] Erik V. Johnstone,[†] Philippe F. Weck,[†,‡] Eunja Kim,[§] Steven D. Conradson,[∥] Alfred P. Sattelberger,[†,‡] and Kenneth R. Czerwinski[†]

[†]Department of Chemistry, University of Nevada Las Vegas, Las Vegas, Nevada 89154, United States

[‡]Sandia National Laboratories, Albuquerque, New Mexico 87185, United States

[§]Department of Physics and Astronomy, University of Nevada Las Vegas, Las Vegas, Nevada 89154, United States

[∥]Materials Science and Technology Division, Los Alamos National Laboratory, Los Alamos, New Mexico 87545, United States

[‡]Energy Engineering and Systems Analysis Directorate, Argonne National Laboratory, 9700 Cass Avenue, Lemont, Illinois 60439, United States

Supporting Information

ABSTRACT: The structure of β-molybdenum dichloride is compared with that of $TcCl_2$ using EXAFS spectroscopy. For $TcCl_2$, the Tc atom is surrounded by Tc atoms at 2.13(2), 3.45(3), 3.79(4), and 4.02(4) Å. For β-$MoCl_2$, the Mo is surrounded by Mo atoms at 2.21(2), 2.91(3), and 3.83(4) Å. The latter distances are consistent with the presence of an $[Mo_4Cl_{12}]$ unit in the solid state, one constituted by two triply Mo−Mo-bonded $[Mo_2Cl_8]$ units. First-principles calculations show that β-$MoCl_2$ with the $TcCl_2$ "structure type" is less stable than α-$MoCl_2$ (Mo_6Cl_{12}) or $[Mo_4Cl_{12}]$ edge-sharing clusters.

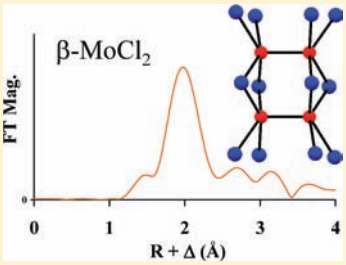

INTRODUCTION

The chemistry of divalent second- and third-row transition metal binary chlorides is underdeveloped, and only a few MCl_2 (M = Zr, Mo, W, Pt, Pd) compounds are known. The coordination chemistry of those dichlorides is dominated by the M_6Cl_{12} (M = Zr, Mo, W, Pt, Pd) cluster.[1a−e] In a recent paper, we described the synthesis of $TcCl_2$ and a new structure type consisting of infinite chains of multiply bonded Tc_2Cl_8 units (Chart 1).[2] It was proposed that the "$TcCl_2$ structure type" might be identified with other metals that are known to form molecular complexes containing the M_2X_8 unit (e.g., M = Mo, W, Re, Os; X = Cl, Br, I). In this context, we were curious about the structure of β-$MoCl_2$.

Chart 1. View of a Technetium Dichloride Chain Along the *c* Axis of the Unit Cell[2]

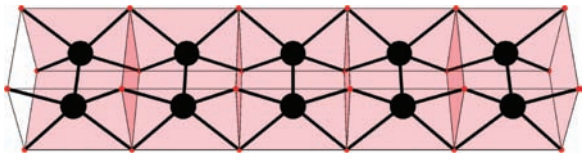

This compound was reported nearly 50 years ago, but its structure is still unknown.[3] It is prepared by reaction of molybdenum(II) acetate, $Mo_2(OAc)_4$, and HCl(g) at 250−350 °C.[4−8] The semicrystalline nature of β-$MoCl_2$ makes its characterization by diffraction techniques difficult. Its broad and diffuse XRD powder pattern resembles that of $CdCl_2$.[4] Earlier work indicated that β-$MoCl_2$ was diamagnetic, suggesting the presence of Mo−Mo bonds, while infrared spectroscopy revealed the presence of Mo−Cl−Mo bridges.[9] Previous experiments showed that it was possible to convert β-$MoCl_2$ to tetranuclear $Mo_4Cl_8(L)_4$ clusters (L= THF, PEt_3). As a result, it was concluded that β-$MoCl_2$ was a polymer containing $[Mo_4Cl_4]$ rectangular clusters coupled by Mo−Cl−Mo bridges, and the formulation $[(Mo_4Cl_4)(Cl_{8/2})]_\infty$ was proposed.[8,9] In this formulation, the tetranuclear clusters are formed by two face-sharing $[Mo_2Cl_8]$ units, which is similar to the arrangement of the Tc_2Cl_8 units in $TcCl_2$ and suggests that β-$MoCl_2$ could have the "$TcCl_2$ structure type". Herein, we report the structures of β-$MoCl_2$ and $TcCl_2$ determined by extended X-ray absorption fine structure spectroscopy (EXAFS).

EXPERIMENTAL SECTION

Caution! Techetium-99 is a weak beta emitter (E_{max} = 292 keV). All manipulations were performed in a radiochemistry laboratory designed for chemical synthesis using efficient HEPA-filtered fume hoods, Schlenk and glovebox techniques, and following locally approved radioisotope handling and monitoring procedures. The starting compound NH_4TcO_4 was purchased from Oak Ridge National Laboratory. Technetium dichloride was prepared according to the method reported in the literature,[2] i.e., reaction between Tc metal and Cl_2(g) (Tc:Cl, 1:2.5) in a sealed tube at 450 °C. The $TcCl_2$ needles produced in the center of the tube were collected and used for EXAFS measurements.

Molybdenum hexacarbonyl and a lecture bottle of HCl(g) were purchased from Sigma-Aldrich. Dimolybdenum tetraacetate was prepared by a variant of the method reported in the literature[10] by

Received: October 17, 2011
Published: April 12, 2012

   dx.doi.org/10.1021/ic202680j | *Inorg. Chem.* 2012, 51, 4965−4971

refluxing molybdenum hexacarbonyl with acetic acid in chlorobenzene under an inert atmosphere. β-$MoCl_2$ was prepared by reaction between $Mo_2(OAc)_4$ and HCl(g) at 300 °C.[4] Molybdenum dichloride was characterized by infrared spectroscopy and XRD powder diffraction. $K_4Mo_2Cl_8 \cdot 2H_2O$ was synthesized from $Mo_2(OAc)_4$ according to a procedure previously reported.[11]

EXAFS Spectroscopy. Measurements were performed at the Advanced Photon Source (APS) at the BESSRC-CAT 12 BM station.[12] The technetium and molybdenum compounds were diluted (~1% by mass) in boron nitride, ground in a mortar, and placed in an aluminum sample holder equipped with Kapton windows. Spectra were recorded at the Tc and Mo Kα edge (21 044 and 20 000 eV) in fluorescence mode at room temperature using a 13-element germanium detector. A double crystal of Si [111] was used as a monochromator. Rejections of harmonics were performed using rhodium mirrors. Energy was calibrated using a molybdenum foil. For each compound, 16 scans were recorded in the k range 0−15 Å^{-1} and averaged. EXAFS spectra were extracted using the Athena[13] software, and data analysis was performed using Winxas.[14] For the fitting procedure, amplitude and phase shift functions were calculated by FEFF 8.2.[15] Input files were generated by Atoms.[16] Simulation studies were performed at $\sigma^2 = 0$; the scattering and amplitude function generated by FEFF 8.2 were extracted, k^3 weighted, and Fourier transformed between k = 2.5 and 14 Å^{-1} using Artemis software.[13]

Computational Methods. First-principles total energy calculations were performed using spin-polarized density functional theory (DFT) as implemented in the Vienna ab initio simulation package (VASP).[17] The exchange-correlation energy was calculated using the generalized gradient approximation (GGA) with the parametrization of Perdew and Wang (PW91).[18,19] The interaction between valence electrons and ionic cores was described by the projector-augmented wave (PAW) method.[20,21] The Tc(4p,5s,4d), Mo(4p,5s,4d), and Cl(3s,3p) electrons were treated explicitly as valence electrons in the Kohn−Sham (KS) equation, and the remaining core electrons together with the nuclei were represented by PAW pseudopotentials. The KS equation was solved using the blocked Davidson iterative matrix diagonalization scheme followed by the residual vector minimization method. The plane-wave cutoff energy for the electronic wave functions was set to a value of 350 eV, ensuring the total energy of the system to be converged to within 1 meV/atom. Electronic relaxation was performed with the conjugate gradient method accelerated using the Methfessel−Paxton Fermi-level smearing[22] with a Gaussian width of 0.1 eV. Ionic relaxation was carried out using the quasi-Newton method, and the Hellmann−Feynman forces acting on atoms were calculated with a convergence tolerance set to 0.01 eV/Å. The Brillouin zone was sampled using the Monkhorst−Pack special k-point scheme[23] with a 3 × 3 × 3 mesh for all structural optimization and total energy calculations.

Other Techniques. An attenuated total reflectance FT-IR (ATR-FT-IR) spectrum of β-$MoCl_2$ was recorded on a Varian Excalibur spectrometer using a KBr beam splitter and an integrated Durasampler diamond ATR. The infrared spectrum does not show any peaks in the region 1300−1600 cm^{-1}, which indicates the absence of Mo(II) acetate in the final product. The XRD powder pattern of β-$MoCl_2$ was recorded on a PANalytical X'Pert Pro instrument with Cu Kα emission and an X'elerator multiple Si strip solid state detector. The XRD powder pattern (Figure S1, Supporting Information) exhibits the characteristic line of β-$MoCl_2$.[4]

RESULTS AND DISCUSSION

EXAFS Spectroscopy. EXAFS spectra of $TcCl_2$, $K_4Mo_2Cl_8 \cdot 2H_2O$, and β-$MoCl_2$ were recorded in fluorescence mode at the Tc and Mo K edges in the k range 0−15 Å^{-1}. EXAFS spectra were k^3 weighted, and the Fourier transforms (FT) were performed in the k range 2.5−14 Å^{-1}. The $\chi(R)$ Fourier transform representations of the EXAFS of β-$MoCl_2$ and $TcCl_2$ (Figure 1) both exhibit a large nearest neighbor peak that, because of the very short M−M bonds, contains the overlapping contributions of the metal and Cl. Beyond this, the more distant neighbor shells display different patterns indicative of different longer range structures for the Mo and Tc compounds.

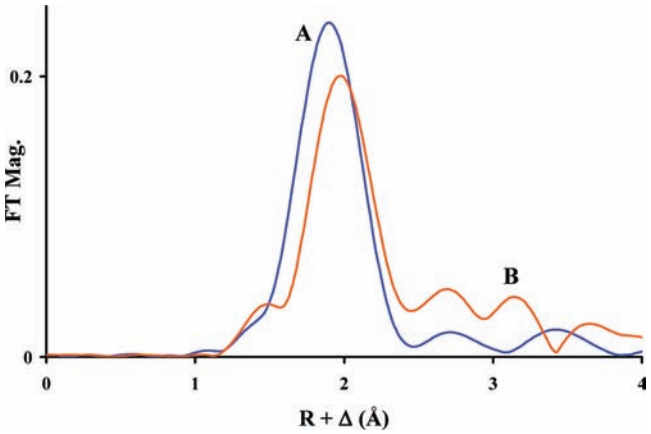

Figure 1. Fourier transform between k = 2.5 and 14 Å^{-1} of the k^3 EXAFS spectra of $TcCl_2$ (A, in blue) and β-$MoCl_2$ (B, in orange).

The unexpected difference in the long-range structures between $TcCl_2$ and β-$MoCl_2$ was initially explored with EXAFS simulations. Modeling the EXAFS of various possible geometries for Tc and Mo chlorides demonstrates the origin of these effects in the Cl bridging geometries (Figure 2 and Figure

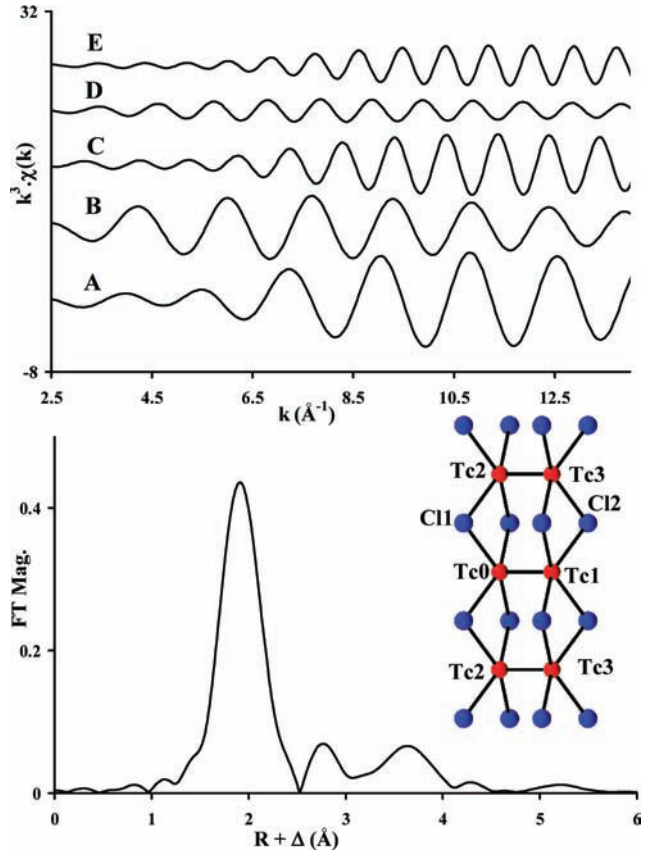

Figure 2. (Top) Individual k^3 EXAFS waves calculated in $TcCl_2$: (A) Tc0 ⇆ Tc1, (B) Tc0 ⇆ Cl1, (C) Tc0 ⇆ Tc2, (D) Tc0 ⇆ Cl2, and (E) Tc0 ⇆ Tc3. (Bottom) Simulated FT and ball-and-stick representations of $TcCl_2$ used for EXAFS calculation. Simulation between k = 2.5 and 14 Å^{-1}.

dx.doi.org/10.1021/ic202680j | Inorg. Chem. 2012, 51, 4965−4971

3). The technetium dichloride EXAFS spectrum was simulated using the structural parameters of a $TcCl_2$ chain derived from its average crystallographic structure.[2] On the simulated FT of $TcCl_2$ (Figure 2, bottom) the first peak corresponds to $Tc_0 \leftrightarrows Tc_1$ and $Tc_0 \leftrightarrows Cl_1$ scattering. For the second peak, $Tc_0 \leftrightarrows Tc_2$ (C) and $Tc_0 \leftrightarrows Cl_2$ (D), the scattering wave functions are in destructive interference mode (Figure 2, top), which results in a low value of the FT magnitude at this distance. The third peak corresponds to $Tc_0 \leftrightarrows Tc_3$ scattering. According to previous studies, β-$MoCl_2$ could exhibit either the $CdCl_2$ or the $[(Mo_4Cl_4)(Cl_{8/2})]_\infty$ structure.[4,8] The EXAFS spectra of β-$MoCl_2$ with the $CdCl_2$[24] structure (Figure S2, Supporting Information) and a postulated Mo_4Cl_{12} structure were calculated for comparison with the experimental data. The structure of Mo_4Cl_{12} (Figure 3, bottom) was derived from the structure of the $Mo_4Cl_8(PEt_3)_4$ complex by replacing the PEt_3 groups with the Cl ligands.[25] The FT of "Mo_4Cl_{12}" (Figure 3, bottom) does capture the features of the experimental spectrum, exhibiting the pattern of two smaller peaks beyond the nearest neighbor contribution above and below R = 3 Å. Metrical information was obtained from the EXAFS by nonlinear, least-squares curve fits that included the single-scattering waves from the five nearest neighbor shells. The Mo−Mo, Tc−Tc, Mo−Cl, and Tc−Cl amplitudes and phases were calculated using the structural parameters of a $TcCl_2$ chain derived from its average crystallographic structure[2] and a postulated Mo_4Cl_{12} cluster.

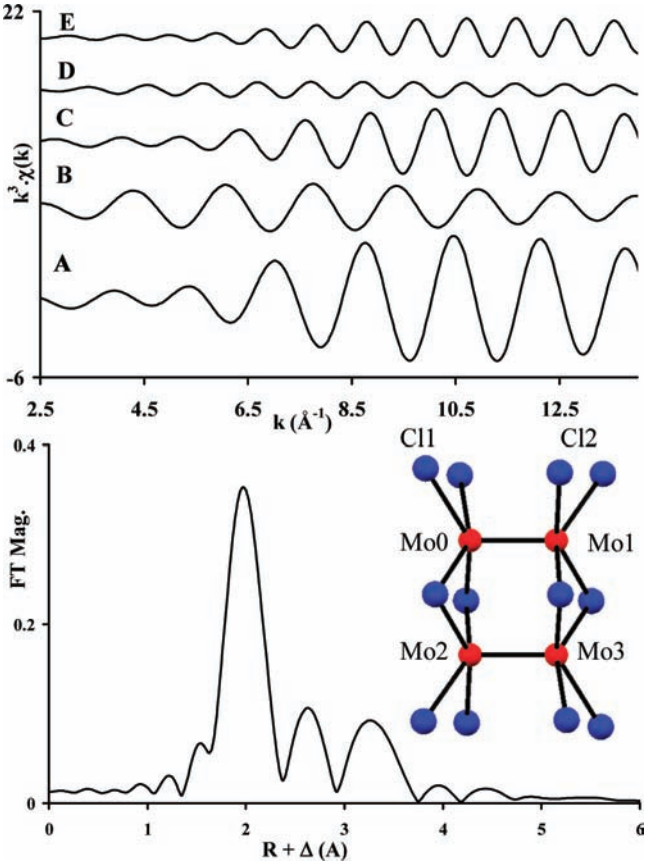

Figure 3. (Top) Individual k^3 EXAFS waves calculated in "Mo_4Cl_{12}": (A) $Mo_0 \leftrightarrows Mo_1$, (B) $Mo_0 \leftrightarrows Cl_1$, (C) $Mo_0 \leftrightarrows Mo_2$, (D) $Mo_0 \leftrightarrows Cl_2$, and (E) $Mo_0 \leftrightarrows Mo_3$. (Bottom) Simulated FT and ball-and-stick representations of the postulated Mo_4Cl_{12} cluster used for EXAFS calculation. Simulation between k = 2.5 and 14 Å^{-1}.

Technetium Dichloride. Adjustment of the k^3-weighted EXAFS spectra was performed in the k range 2.5−14 Å^{-1} under the constraints S_0^2 = 0.9. The adjustment procedure was initially conducted using the scattering functions previously mentioned. The multiscattering $Cl_1 \leftrightarrows Tc_0 \leftrightarrows Cl_1$ was used to fit the peak located at $R + \Delta$ = 4.2 Å. ΔE_0 was constrained to be the same value for each wave. The numbers of atoms were fixed at those of the crystal structure; this places all of the amplitude variation in the Debye−Waller factors, which nevertheless are well behaved in that they increase monotonically with distance. The errors in distances are within the normal 0.02 Å for nearest neighbors and 0.03−0.05 Å for the more distant ones whose contributions overlap to an unusually large extent.

The fitted FT and the k^3 EXAFS spectra are shown in Figure 4. The residual, i.e., the difference between the adjustment and experimental data is 4.80%. The structural parameters (Table 1) found by EXAFS indicate the environment around Tc_0 to consist of Tc atoms at 2.13(2), 3.48(3), and 4.08(4) Å and of Cl atoms at 2.42(2) and 3.59(4) Å.

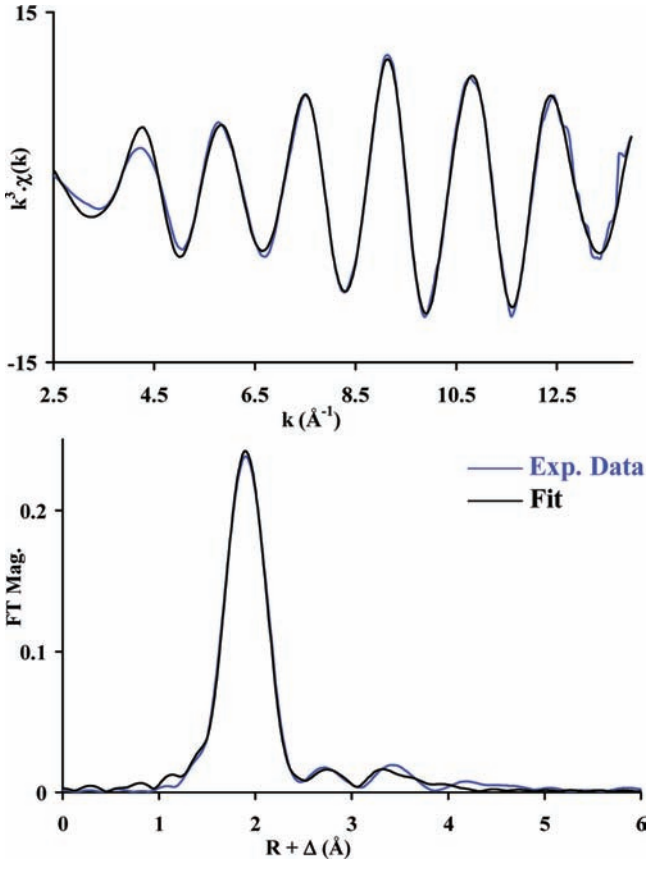

Figure 4. Fitted experimental k^3 EXAFS spectra (top) and Fourier transform of k^3 EXAFS spectra (bottom) of $TcCl_2$. Adjustment between k = 2.5−14 Å^{-1}. Experimental data (blue) and fit (black).

The $TcCl_2$ sample used for the XRD structure determination[2] was thermally treated at 450 °C with $AlCl_3$ while the sample used in the present work was not. The absence of thermal treatment with $AlCl_3$ could introduce disorder within the structure, such as perpendicular orientations of the Tc≡Tc vectors in a $TcCl_2$ chain. In order to investigate the presence of perpendicular orientations of the Tc≡Tc vectors, a fourth shell

dx.doi.org/10.1021/ic202680j | Inorg. Chem. 2012, 51, 4965−4971

Table 1. Structural Parameters Obtained by Adjustment of the k^3 EXAFS Spectra of $TcCl_2$[a]

scattering	C.N.	R (Å)	σ^2 (Å^2)
$Tc_0 \leftrightarrows Tc_1$	1	2.13(2), *2.129(1), 2.129(1)*	0.0017(9)
$Tc_0 \leftrightarrows Cl_1$	4	2.42(2), *2.391(2), 2.391(2)*	0.0036(15)
$Tc_0 \leftrightarrows Tc_2$	2	3.48(3), *3.417(2), 3.417(2)*	0.0057(20)
$Tc_0 \leftrightarrows Cl_2$	4	3.60(4), *3.532(1), 3.532(1)*	0.0072(27)
$Tc_0 \leftrightarrows Tc_3$	2	4.09(4), *4.025(2), 4.025(2)*	0.0093(25)

[a]The adjustment was performed using the scattering calculated from the model presented in Figure 2. Adjustment between k = 2.5−14 Å^{-1}. ΔE_0 = 2.43 eV. S_0^2 = 0.9. The values found by XRD are in italics.

of Tc atoms (i.e., Tc_4) was considered for the EXAFS adjustment. The model used for the EXAFS calculation (Figure 5) was constructed considering three adjacent Tc_2Cl_8 units with

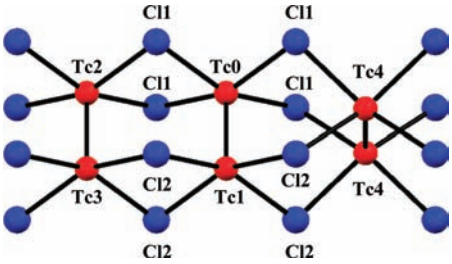

Figure 5. Ball and stick representation of the model used for EXAFS calculations considering parallel and perpendicular Tc≡Tc vectors.

perpendicular and parallel Tc≡Tc vectors. The structural parameters of the Tc_2Cl_8 units in this model were taken from the one determined in the published $TcCl_2$ X-ray structure.[2] In this model, the Tc_0−Tc_4 distance is 3.734(2) Å. For the fitting procedure, the numbers of atoms were fixed at those of the model; the fitted FT and the k^3 EXAFS spectra are shown in Figure 6. The structural parameters (Table 2) found by EXAFS indicate the environment around Tc_0 consists of Tc atoms at 2.13(2), 3.45(3), 3.79(4), and 4.02(4) Å and of Cl atoms at 2.42(2) and 3.58(4) Å. The value of the residual (3.80%) is lower than the one previously found while the Tc_0−Tc_2 and Tc_0−Tc_3 distances are closer to the ones reported by XRD (Table 2). The presence of Tc atoms at 3.79(4) and 3.45(3) Å indicates that the structure of $TcCl_2$, produced by the reaction of Tc metal and elemental chlorine consists of face sharing Tc_2Cl_8 units, with two orientations of the Tc≡Tc vectors, i.e., the Tc≡Tc vectors of two adjacent Tc_2Cl_8 units are either parallel or perpendicular. In order to confirm these results, further crystallographic experiments are in progress and will be reported in due course.

Potassium Octachlorodimolybate. The EXAFS spectrum of $K_4Mo_2Cl_8{\cdot}2H_2O$ was studied in order to validate our approach in the determination of metal−metal bond lengths in β-$MoCl_2$. The EXAFS spectrum of $K_4Mo_2Cl_8{\cdot}2H_2O$ was fit using the scattering functions calculated from its crystallographic structure.[26] Two adjustments were performed: (1) Fourier filtering was performed between $R + \Delta$ = 1.20 and 2.30 Å, the FT was back-transformed, and the corresponding EXAFS spectra fitted in the k range 2.5−14 Å^{-1}; (2) adjustment of the total EXAFS spectra in the k range 2.5−14 Å^{-1}. For both adjustments, ΔE_0 was constrained to be the same value for each wave, and the numbers of atoms were fixed at those of the crystal structure. The structural parameters found in adjustment **2** (Figure 7, Table 3) indicate the environment of the absorbing

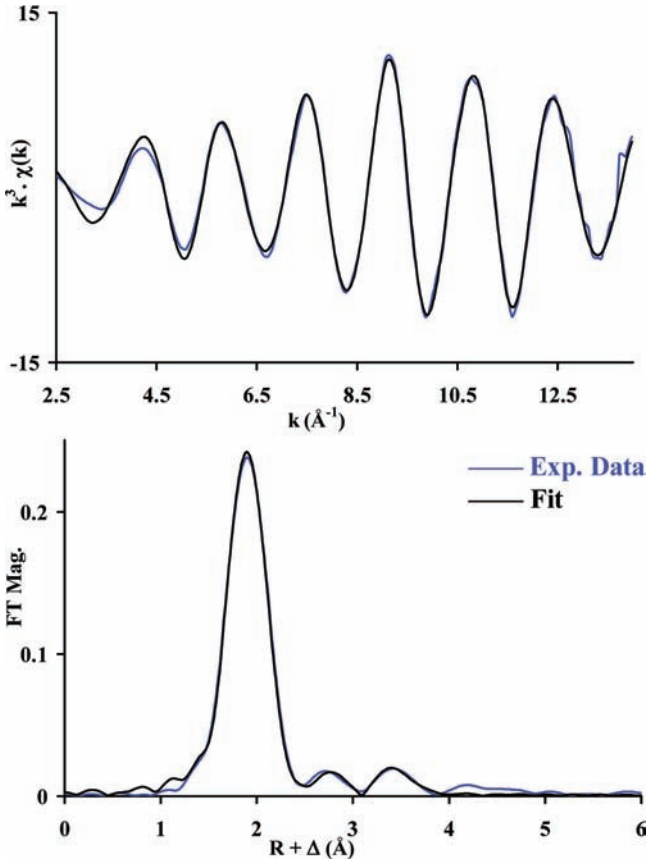

Figure 6. Fitted experimental k^3 EXAFS spectra (top) and Fourier transform of k^3 EXAFS spectra (bottom) of $TcCl_2$. Adjustment between k = 2.5−14 Å^{-1}. Experimental data (blue) and fit (black).

Table 2. Structural Parameters Obtained by Adjustment of the k^3 EXAFS Spectra of $TcCl_2$[a]

scattering	C.N.	R (Å)	σ^2 (Å^2)
$Tc_0 \leftrightarrows Tc_1$	1	2.13(2)	0.0019(9)
$Tc_0 \leftrightarrows Cl_1$	4	2.42(2)	0.0035(15)
$Tc_0 \leftrightarrows Tc_2$	1	3.45(3), *2.139(4)*	0.0043(19)
$Tc_0 \leftrightarrows Cl_2$	4	3.58(4)), *2.45[2]*	0.0079(27)
$Tc_0 \leftrightarrows Tc_3$	1	4.02(4), *3.65[2]*	0.0084(25)
$Tc_0 \leftrightarrows Tc_4$	2	3.79(4), *4.00[2]*	0.0062(21)

[a]The adjustment was performed used the scattering calculated in the model presented in Figure 5. The adjustment is between k = 2.5−14 Å^{-1}. ΔE_0 = 1.82 eV. S_0^2 = 0.9.

atom to be constituted by one Mo atom at 2.16(2) Å, four Cl atoms at both 2.44(2) and 3.69(4) Å, and two K atoms at 4.05(4) Å. Due to the weak scattering amplitude and large distance from the absorbing atom (Tc···O = 4.75 Å), the oxygen atoms from the water molecules were not considered for the adjustment. These structural parameters are essentially identical to those found in the X-ray structure of $K_4Mo_2Cl_8{\cdot}2H_2O$ and validate our approach.

β-Molybdenum Dichloride. Adjustment was conducted similarly to the one performed for $K_4Mo_2Cl_8{\cdot}2H_2O$. The adjustment of the experimental EXAFS spectra was performed in the k range 2.5−14 Å^{-1} using the calculated scattering wave functions determined from the postulated Mo_4Cl_{12} cluster. Attempts to adjust the EXAFS spectra of β-$MoCl_2$ using the structure of $TcCl_2$ were unsuccessful. Two adjustments were

dx.doi.org/10.1021/ic202680j | Inorg. Chem. 2012, 51, 4965−4971

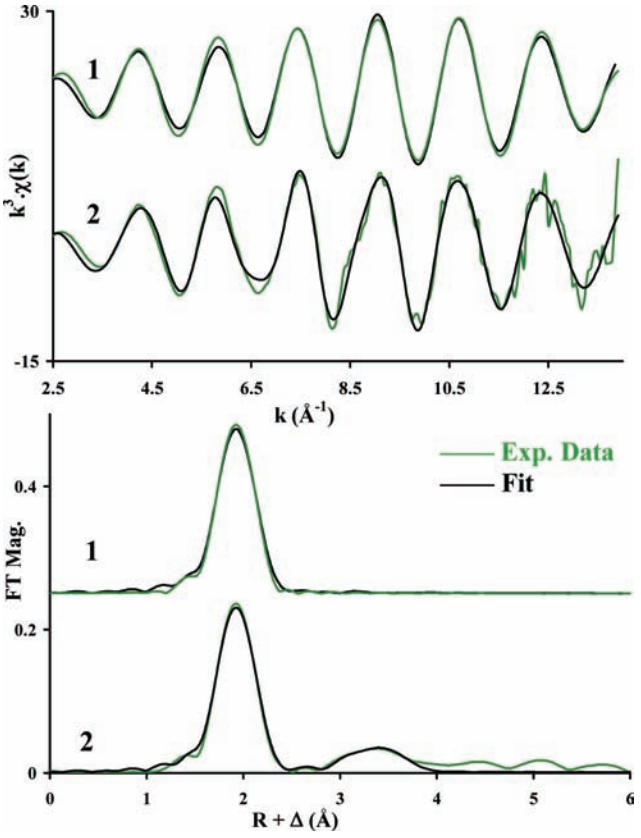

Figure 7. Fitted experimental k^3 EXAFS spectra (top) and Fourier transform of k^3 EXAFS spectra (bottom) of $K_4Mo_2Cl_8{\cdot}2H_2O$. Experimental data (orange) and fit (black). Adjustment performed between k = 2.5 and 14 Å^{-1}.

Table 3. Structural Parameters Obtained by Adjustment of the k^3 EXAFS Spectra of $K_4Mo_2Cl_8{\cdot}2H_2O$[a]

adjustment	scattering	C.N.	R (Å)	σ^2 (Å^2)
1	$Mo_0 \leftrightarrows Mo_1$	1	2.16(2)	0.0016(9)
	$Mo_0 \leftrightarrows Cl_1$	4	2.45(2)	0.0048(17)
2	$Mo_0 \leftrightarrows Mo_1$	1	2.16(2), 2.139(4)	0.0016(9)
	$Mo_0 \leftrightarrows Cl_1$	4	2.44(2), *2.45[2]*	0.0048(17)
	$Mo_0 \leftrightarrows Cl_2$	4	3.69(4), *3.65[2]*	0.00369(25)
	$Mo_0 \leftrightarrows K$	2	4.05(4), *4.00[2]*	0.0060(24)

[a]Adjustment **1** and **2** performed between k = 2.5 and 14 Å^{-1}. ΔE_0 = 3.36 eV (**1**) and 3.83 eV (**2**). S_0^2 = 0.9. The values found by XRD are in italic.

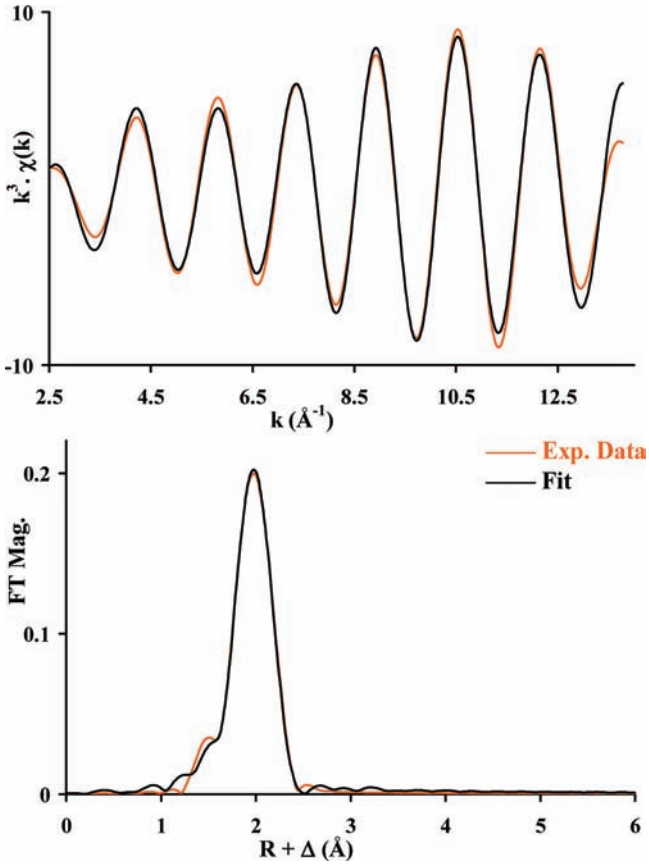

Figure 8. Adjustment of the filtered Fourier transform (bottom) and back-transformed k^3 EXAFS (top) spectra of β-$MoCl_2$. Experimental data (orange) and fit (black). Fourier Filtering between R + ΔR = 1.20−2.30 Å; adjustment between k = 2.5 and 14 Å^{-1}.

Table 4. Structural Parameters Obtained by Adjustment of the k^3 EXAFS Spectra of β-$MoCl_2$[a]

adjustment	scattering	C.N.	R (Å)	σ^2 (Å^2)
1	$Mo_0 \leftrightarrows Mo_1$	1	2.21(2)	0.0016(9)
	$Mo_0 \leftrightarrows Cl_1$	4	2.48(2)	0.0057(15)
2	$Mo_0 \leftrightarrows Mo_1$	1	2.21(2)	0.0017(9)
	$Mo_0 \leftrightarrows Cl_1$	4	2.46(2)	0.0050(15)
	$Mo_0 \leftrightarrows Mo_2$	1	2.91(3)	0.0036(12)
	$Mo_0 \leftrightarrows Cl_1$	4	3.63(4)	0.0054(20)
	$Mo_0 \leftrightarrows Mo_3$	1	3.83(4)	0.0080(30)

[a]Adjustment **1** and **2** performed between k = 2.5 and 14 Å^{-1}. ΔE_0 = 6.01 (**1**) and 2.85 eV (**2**). S_0^2 = 0.9.

performed: (1) Fourier filtering was performed between R+ Δ = 1.20 and 2.30 Å, the FT was back-transformed, and the corresponding EXAFS spectra fitted in the k range 2.5−14 Å^{-1}; (2) adjustment of the total EXAFS spectra in the k range 2.5−14 Å^{-1}. For both adjustments, ΔE_0 was constrained to be the same value for each wave.

Adjustment (1) between R + Δ = 1.20 and 2.30 Å. A window filter was done on the FT between R + Δ = 1.20 and 2.30 Å. The FT was back-transformed, and the corresponding EXAFS spectra were fitted in the k range 2.5−14 Å^{-1} using the Mo0 ⇆ Mo1 and Mo0 ⇆ Cl1 scattering. The results (Figure 8, Table 4) of the adjustment indicate that the first coordination shell around the absorbing atom is constituted by one Mo atom at 2.21(2) Å and four Cl atoms at 2.48(2) Å. These results are in agreement with the presence of the $[Mo_2Cl_8]$ unit in β-$MoCl_2$.

Adjustment (2) of the Total EXAFS Spectra. The total EXAFS spectrum was fitted in thr k range 2.5 and 14 Å^{-1} using the scattering Mo0 ⇆ Mo1, Mo0 ⇆ Cl1, Mo0 ⇆ Mo2, Mo0 ⇆ Cl2, and Mo ⇆ Mo3. The C.N. numbers were fixed to the theoretical value; all other parameters were allowed to vary. The residual (difference between the adjustment and the experimental data) is 6.42%. The results of the final adjustment (Figure 9, Table 4) indicate the environment around Mo_0 consists of Mo atoms at 2.21(2), 2.91(3), and 3.83(4) Å by 4 Cl atoms at 2.46(2) Å and 4 Cl atoms at 3.63(4) Å.

The Mo cluster therefore consists of two face-sharing $[Mo_2Cl_8]$ units, which gives a rectangular $[Mo_4]^{8+}$ core. The

dx.doi.org/10.1021/ic202680j | Inorg. Chem. 2012, 51, 4965−4971

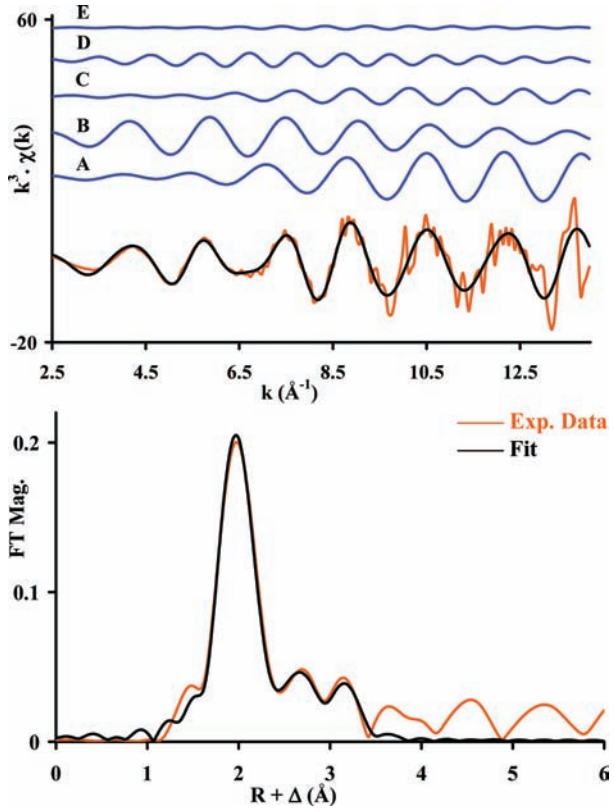

Figure 9. Fitted experimental k^3 EXAFS spectra (top) and Fourier transform of k^3 EXAFS spectra (bottom) of β-$MoCl_2$. Experimental data (orange) and fit (black). Individual separate EXAFS contributions are represented in blue (top): (A) $Mo_0 \leftrightarrows Mo_1$, (B) $Mo_0 \leftrightarrows Cl_1$, (C) $Mo_0 \leftrightarrows Mo_2$, (D) $Mo_0 \leftrightarrows Cl_2$, and (E) $Mo_0 \leftrightarrows Mo_3$. Adjustment performed between k = 2.5 and 14 Å^{-1}.

presence of Mo atoms at 3.83(4) Å indicates the cluster is connected to other clusters through bridging chlorines (see Computational Studies). The Mo−Mo distance in the $[Mo_2Cl_8]$ units, 2.21(2) Å, is larger than that in the $Mo_2Cl_8^{4-}$ anions (2.123(2)−2.139(4) Å)[27] and suggests that the quadruple bond is lost during formation of β-$MoCl_2$. The distance between the Mo atoms bridged by Cl ligands ($Mo(\mu\text{-}Cl)_2Mo$ = 2.91(3) Å) is shorter than the nonbonding Mo···Mo distances (i.e., ∼3.60 Å) and suggests there is a metal−metal bonding interaction between the chloride-bridged Mo atoms.[27,28]

The structure and bonding in Mo tetramers with rectangular cores has been discussed previously.[27−30] For tetramers such as $Mo_4Cl_8(PEt_3)_4$, the Mo−Mo and $Mo(\mu\text{-}Cl)_2Mo$ distances are 2.21 and 2.91 Å and triple and single bonds have been proposed.[28−30] The absence of the δ bond in this type of compound was supported by the absence of the band associated with a $\delta \rightarrow \delta^*$ transition in their electronic spectra.[29]

The similarity of distances between $Mo_4Cl_8(PEt_3)_4$ and β-$MoCl_2$ is consistent with the presence of a triple bond in the $[Mo_2Cl_8]$ unit and a single bond in $Mo(\mu\text{-}Cl)_2Mo$. Additional theoretical calculations estimate a Mo−Mo triple bond at 2.26 Å and Mo−Mo single bond at 2.76 Å.[31]

Computational Studies. In order to better understand the structure observed in the $MoCl_2$ system, total energy calculations of idealized 3D periodic $MoCl_2$ models adopting the α-$MoCl_2$-, $TcCl_2$-, and Mo_4Cl_{12}-type structures have been performed; several crystalline structures based on edge- and corner-sharing Mo_4Cl_{12} building blocks have also been investigated (Figure S3, Supporting Information). The computed total energy per formula unit shows that α-$MoCl_2$ (Mo_6Cl_{12}) is the most stable structure (E = −17.47 eV/fu; Figure S3(a), Supporting Information), followed by the structure with edge-sharing $[Mo_4Cl_{12}]$ clusters (Figure 10)

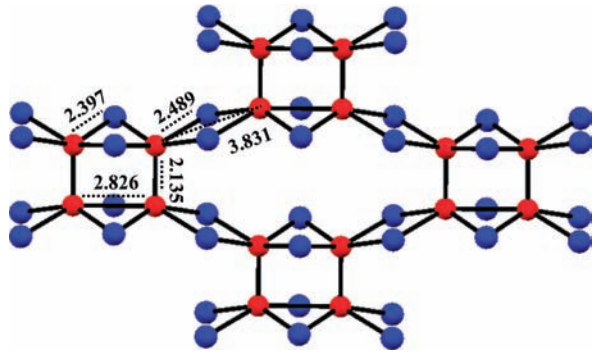

Figure 10. Ball-and-stick representation of the β-$MoCl_2$ structure with edge-sharing $[Mo_4Cl_{12}]$ clusters, with only parallel orientation of the Mo tetranuclear clusters, relaxed using DFT at the GGA/PW91 level of theory with the projector augmented wave method.

with only a parallel orientation of the Mo tetranuclear clusters (E = −17.30 eV/fu); a structure similar to the latter but with both parallel and perpendicular orientations of the Mo tetranuclear clusters appears to be slightly less energetically favorable [E = −17.22 eV/fu; Figure S3(c), Supporting Information]. The $MoCl_2$ model with the $TcCl_2$-type structure made of face-sharing $[Tc_2Cl_8]$ units is significantly less stable [E/fu = −17.17 eV; Figure S3(d), Supporting Information], although it is energetically more favorable than candidate structures with corner-sharing $[Mo_4Cl_{12}]$ clusters [Figure S3(e) and S3(f), Supporting Information]. In agreement with our theoretical results, previous studies have shown that β-$MoCl_2$ was converted to Mo_6Cl_{12} after thermal treatment.[6]

The computed bond lengths in α-$MoCl_2$ are 2.61 Å for Mo−Mo and 2.40, 2.49, and 2.54 Å for Mo−Cl, in excellent agreement with experimental values.[32] In the relaxed structure with edge-sharing $[Mo_4Cl_{12}]$ clusters shown in Figure 10, the Mo−Mo bond distances are 2.14 and 2.83 Å and the Mo−Cl bond distances are 2.40 Å for the Cl atoms bridging the Mo atoms forming the tetranuclear clusters and 2.49 Å for the Cl atoms bridging the $[Mo_4Cl_{12}]$ units. While the calculated Mo−Mo bond lengths forming the Mo tetranuclear are slightly shorter than the average distances of 2.21(2) and 2.91(3) Å determined from EXAFS, their computed bond length ratio of 1.32 reproduces the experimental value of 1.32(3). The calculated average Mo−Cl bond length of ca. 2.45 Å is also consistent with the distance of 2.46(2) Å derived from EXAFS.

■ CONCLUSION

In summary, β-$MoCl_2$ and $TcCl_2$ have been synthesized and their structures analyzed by EXAFS spectroscopy. Results for technetium confirm that $TcCl_2$ is comprised of face-sharing $[Tc_2Cl_8]$ units. For β-$MoCl_2$, EXAFS results are consistent with the presence of an $[Mo_4Cl_{12}]$ cluster. In the cluster constituted by two face-sharing $[Mo_2Cl_8]$ units, the $Mo(\mu\text{-}Cl)_2Mo$ separations indicate metal−metal interactions between the $[Mo_2Cl_8]$ units. Distances are consistent with the presence of a triple bond in $[Mo_2Cl_8]$ and a single bond in $Mo(\mu\text{-}Cl)_2Mo$.

dx.doi.org/10.1021/ic202680j | Inorg. Chem. 2012, 51, 4965−4971

Calculations in the $MoCl_2$ system confirm that α-$MoCl_2$ or Mo_6Cl_{12} is the most stable structure while $MoCl_2$ with a $TcCl_2$ structure is less stable than $MoCl_2$ constituted by Mo_4Cl_{12} bridging clusters. Molybdenum is the third transition metal where a multiple-bonded binary chloride has been synthesized from reaction between a multiple metal−metal-bonded dimer with HCl(g).[7,33] Binary dichlorides of group VIII are still unknown. It will be interesting to see if $RuCl_2$ can be synthesized by reaction between $Ru_2(O_2CCH_3)_4(H_2O)_2$ and HCl(g).[33,34]

■ ASSOCIATED CONTENT

Supporting Information

X-ray powder diffraction of β-$MoCl_2$ and additional computational and EXAFS figures. This material is available free of charge via the Internet at http://pubs.acs.org.

■ AUTHOR INFORMATION

Corresponding Author

*E-mail: poineauf@unlv.nevada.edu.

Notes

The authors declare no competing financial interest.

■ ACKNOWLEDGMENTS

Funding for this research was provided by an NEUP grant "Development of Alternative Technetium Waste Forms" from the U.S. Department of Energy, Office of Nuclear Energy, through INL/BEA, LLC, 89445. Use of the Advanced Photon Source at Argonne was supported by the U.S. Department of Energy, Office of Science, Office of Basic Energy Sciences, under Contract No. DE-AC02-06CH11357. Sandia National Laboratories is a multiprogram laboratory operated by Sandia Corp., a wholly owned subsidiary of Lockheed Martin Co., for the United States Department of Energy's National Nuclear Security Administration under Contract DE-AC04-94AL85000. The work at LANL was supported by the DOE OBES Heavy Element Chemistry Program. The authors thank Mr. Tom O'Dou, Trevor Low, and Julie Bertoia for outstanding health physics support and Dr. Sungsik Lee at the APS for outstanding support during EXAFS experiment.

■ REFERENCES

(1) (a) Schäfer, H.; Schnering, H. G.; Tillack, J.; Kuhnen, F.; Woehrle, H.; Baumann, H. *Z. Anorg. Allg. Chem.* **1967**, *353*, 281−310. (b) Weisser, M.; Tragl, S.; Meyer, H. J. *J. Cluster Sci.* **2009**, *20*, 249−258. (c) Imoto, H.; Corbett, J. D.; Cisar, A. *Inorg. Chem.* **1981**, *20*, 145−151. (d) Brodersen, K.; Thiele, G.; Schnering, H. G. *Z. Anorg. Allg. Chem.* **1965**, *337*, 120−127. (e) Schäfer, H.; Wiese, U.; Rinke, K.; Brendel, K. *Angew. Chem., Int. Ed.* **1967**, *6*, 253−254.

(2) Poineau, F.; Malliakas, C. D.; Weck, P. F.; Scott, B. L.; Johnstone, E. V.; Forster, P. M.; Kim, E.; Kanatzidis, M. G.; Czerwinski, K. R.; Sattelberger, A. P. *J. Am. Chem. Soc.* **2011**, *133*, 8814−8817.

(3) Stephenson, T. A.; Bannister, E.; Wilkinson, G. *J. Chem. Soc.* **1964**, 2538−2541.

(4) Allison, G. B.; Anderson, I. R.; Sheldon, J. C. *Aust. J. Chem.* **1969**, *22*, 1091−1095.

(5) Hamer, A. D.; Walton, R. A. *Inorg. Chem.* **1974**, *13*, 1446−1451.

(6) Holste, G.; Schaefer, H. *J. Less-Common Met.* **1970**, *20*, 164−166.

(7) Glicksman, H. D.; Hamer, A. D.; Smith, T. J.; Walton, R. A. *Inorg. Chem.* **1976**, *15*, 2205−2209.

(8) Beers, W. W.; McCarley, R. E. *Inorg. Chem.* **1985**, *24*, 472−475.

(9) Ryan, T. R.; McCarley, R. E. *Inorg. Chem.* **1982**, *21*, 2072−2079.

(10) Brignole, A. B.; Cotton, F. A. *Inorg. Synth.* **1972**, *13*, 81.

(11) Brencic, J. V.; Cotton, F. A. *Inorg. Chem.* **1970**, *9*, 351−353.

(12) Beno, M. A.; Engbretson, M.; Jennings, G.; Knapp, G. S.; Linton, J.; Kurtz, C.; Rutt, U.; Montano, P. A. *Nucl. Instrum. Methods A* **2001**, *467−468*, 699−702.

(13) Ravel, B.; Newville, M. *J. Synchrotron Radiat.* **2005**, *12*, 537−541.

(14) Ressler, T. *J. Synchrotron Radiat.* **1998**, *5*, 118−122.

(15) Rehr, J. J.; Albers, R. C. *Rev. Mod. Phys.* **2000**, *72*, 621−654.

(16) Ravel, B. *J. Synchrotron Radiat.* **2001**, *8*, 314−316.

(17) Kresse, G.; Furthmüller, J. *Phys. Rev. B* **1996**, *54*, 11169−11186.

(18) Perdew, J. P.; Chevary, J. A.; Vosko, S. H.; Jackson, K. A.; Pederson, M. R.; Singh, D. J.; Fiolhais, C. *Phys. Rev. B* **1992**, *46*, 6671−6687.

(19) Perdew, J. P.; Wang, Y. *Phys. Rev. B* **1992**, *45*, 13244−13249.

(20) Blöchl, P. E. *Phys. Rev. B* **1994**, *50*, 17953−17979.

(21) Kresse, G.; Joubert, D. *Phys. Rev. B* **1999**, *59*, 1758−1175.

(22) Methfessel, M.; Paxton, A. T. *Phys. Rev. B* **1989**, *40*, 3616−3621.

(23) Monkhorst, H. J.; Pack, J. D. *Phys. Rev. B* **1976**, *13*, 5188−5192.

(24) Knop., O. *J. Solid. State. Chem.* **1982**, *45*, 223−234.

(25) Cotton, F. A.; Shang, M. *J. Clust. Sci.* **1991**, *2*, 121−129.

(26) Brencic, J. V.; Cotton, F. A. *Inorg. Chem.* **1969**, *8*, 7−10.

(27) Cotton, F. A. In *Multiple Bonds between Metal Atoms*, 3rd ed.; Cotton, F. A., Murillo, C. A., Walton, R. A., Eds.; Springer, New York, 2005; Chapter 4.

(28) Cotton, F. A.; Daniels, L. M.; Guimet, I.; Henning, R. W.; Jordan, G. T.; Lin, C.; Murillo, C. A.; Schultz, A. J. *J. Am. Chem. Soc.* **1998**, *120*, 12531−12538.

(29) McGinnis, R. N.; Ryan, T. R.; McCarley, R. E. *J. Am. Chem. Soc.* **1978**, *100*, 7900−7902.

(30) Chisholm, M. H.; Macintosh, A. M. *Chem. Rev.* **2005**, *105*, 2949−2976.

(31) Pyykko, P.; Atsumi, M. *Chem.—Eur. J.* **2009**, *15*, 12770−12779.

(32) von Schnering, H. G.; May, W.; Peters, K. *Z. Kristallog.* **1993**, *208*, 368−369.

(33) Poineau, F.; Johnstone, E. V.; Weck, P. F.; Kim, E.; Forster, P. M.; Scott, B. L.; Sattelberger, A. P.; Czerwinski, K. R. *J. Am. Chem. Soc.* **2010**, *132*, 15864−15865.

(34) Lindsay, A. J.; Wilkinson, G.; Motevalli, M.; Hursthouse, M. B. *J. Chem. Soc., Dalton Trans.* **1985**, *11*, 2321−2326.